Am J Transl Res 2018;10(8):2480-2490
www.ajtr.org /ISSN:1943-8141/AJTR0073076

Original Article

E7 peptide-functionalized Ti6Al4V alloy for BMSC enrichment in bone tissue engineering

Zhentao Man, Tao Li, Laibo Zhang, Lin Yuan, Changshun Wu, Ping Li, Shui Sun, Wei Li

Department of Joint Surgery, Shandong Provincial Hospital Affiliated to Shandong University, Jinan 250021, Shandong Province, P. R. China

Received January 19, 2018; Accepted July 29, 2018; Epub August 15, 2018; Published August 30, 2018

Abstract: Ti6Al4V alloy is widely used for hip joint prostheses, however owing to its lack of biomimetic surface properties, it often suffers from poor osseointegration. It is well known that bone mesenchymal stem cells (BMSCs) play an important role in the osseointegration of the host bone and joint prostheses. One promising approach to improving the osseointegration of joint prostheses is to enrich the number of BMSCs at the periprosthetic site. Previous studies have reported that BMSC specific affinity peptide E7, can specifically enrich BMSCs. However, to date, few studies have reported the use of E7 in bone tissue engineering. In this study, we conjugated E7 peptide to Ti6Al4V alloy to fabricate a scaffold (BTS) to improve the biocompatibility of the alloy. E7 peptide efficiently improved the adhesion of BMSCs to Ti6Al4V alloy. In addition, the BTS scaffold was more conducive to osteogenesis than the RGD-functionalized and non-functionalized control scaffolds. The functional BTS scaffold could pave the way for designing functional joint prostheses, which promote osseointegration between the host bone and implant.

Keywords: Bone tissue engineering, BMSCs, specific affinity peptide, Ti6Al4V alloy, covalent cross-linking

Introduction

Ti6Al4V alloy (titanium, 6% aluminum, 4% vanadium) is widely used for hip joint prostheses because of its proven biocompatibility and mechanical properties [1]. However, the surface of Ti6Al4V alloy is not biomimetic, which often leads to poor osseointegration between the host bone and joint prostheses [2]. Poor osseointegration can lead to looseness of joint prostheses, which is a catastrophic complication for total hip arthroplasty. Reducing the incidence of prosthesis looseness through bio-functionalization of Ti6Al4V alloy to promote osseointegration, is therefore an area of focused research in bone tissue engineering.

To date, the bio-functionalization of Ti6Al4V alloy has mainly focused on surface modification. The surface modification of Ti6Al4V alloy can be divided into two approaches: one approach is using bioactive coatings, such as RGD coating [1], or calcium phosphate coating [3]; the other is physicochemical modification of the alloy, such as changes to surface roughness [2, 4]. The RGD peptide has been widely studied because of its cell attachment. For example, Mas-Moruno et al. reported that the RGD peptide could efficiently enhance osteoblast adhesion to the surface of Ti6Al4V alloy [1]. The RGD peptide comprises an arginine-glycine-aspartate amino acid sequence, which is prevalent in the extracellular matrix and is responsible for the initial attachment of various cells [5]. As a result, in addition to promoting seed cells, RGD peptide can also enrich the concentration of inflammatory cells at the surface of Ti6Al4V alloy [6], which could adversely affect osseointegration.

It is well known that bone mesenchymal stem cells (BMSCs) play an important role in the osseointegration between the host bone and implant surface because osteoblasts at the periprosthetic site are differentiated from BMSCs [7]. Therefore, one promising method for improving the osseointegration between the host bone and implant, is to enrich the concentration of BMSCs at the periprosthetic site [8]. In addition, the greater adhesion efficiency of

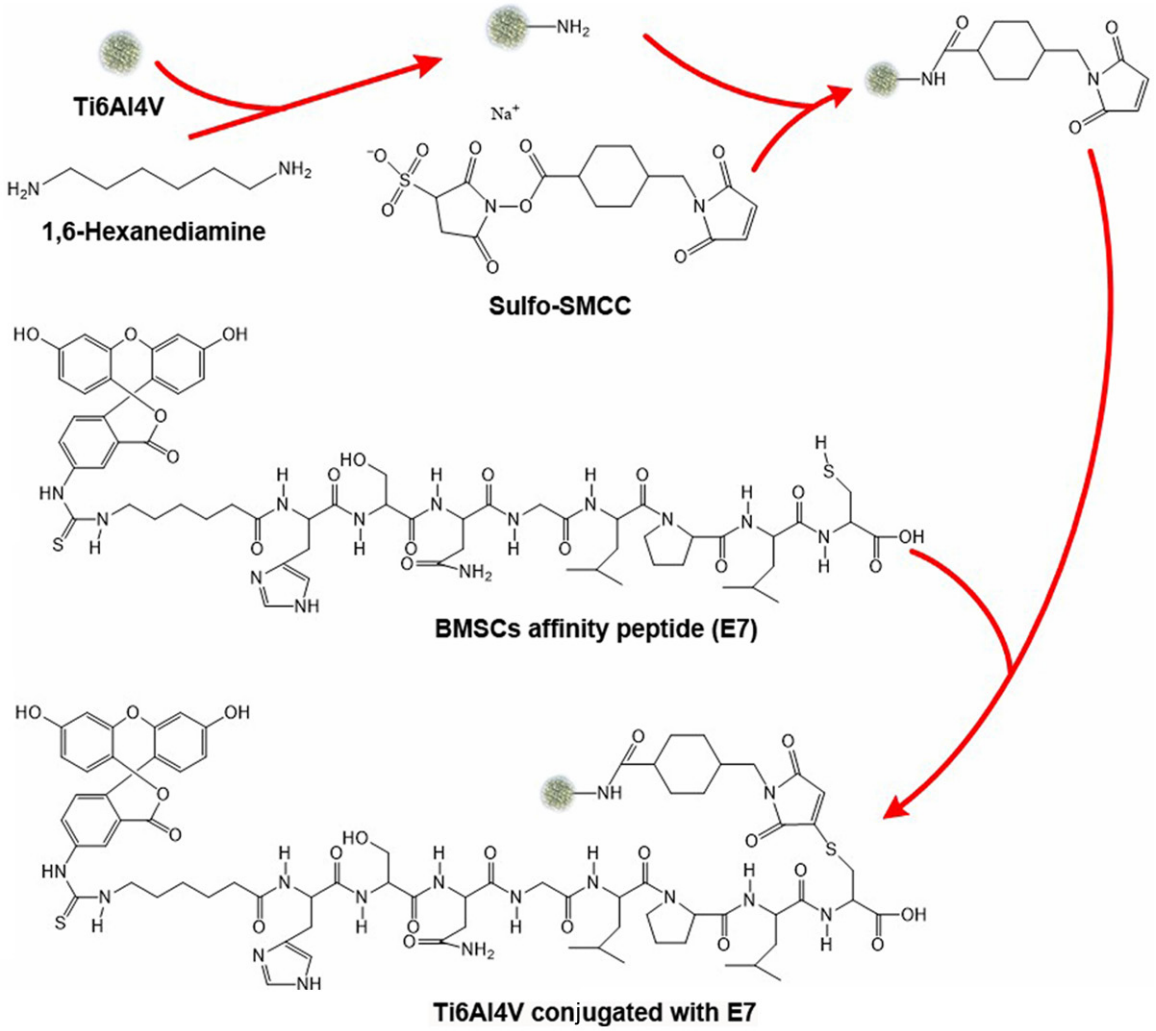

Figure 1. Schematic illustration of the covalent conjugation of the BMSC affinity peptide (E7) to the Ti6Al4V scaffold using the Sulfo-SMCC crosslinker.

BMSCs could reduce the rate of infection, which can be a catastrophic complication for hip arthroplasty [9]. Gristina has reported that, immediately following the implantation of a prosthesis in hip arthroplasty, a "race for the surface" between bacteria and tissue cells takes place [10]. If bacteria win the race, hip periprosthetic joint infection may occur. Therefore, a biomimetic prosthesis surface that supports the adhesion of seed cells during the "race for the surface" could decrease the infection rate and promote osseointegration [11].

In a previous study, Shao et al. reported the effects of the BMSC specific affinity peptide E7 (a peptide sequence composed of seven amino acids: EPLQLKM), which could specifically and effectively facilitate the adhesion of BMSCs to electrospun mesh [6]. Interestingly, the E7 peptide promoted the development of fewer inflammatory cells than the RGD peptide, indicating that the E7 peptide causes less inflammation damage. However, to date, few studies have reported the use of E7 in bone tissue engineering. In this study, we conjugated E7 peptide to Ti6Al4V alloy to investigate whether E7 could enrich BMSCs on a Ti6Al4V alloy surface and promote osseointegration between the alloy and host bone.

In brief, the aim of this study was to develop E7-modified Ti6Al4V alloy to promote BMSC recruitment and osseointegration, using pure Ti6Al4V alloy and RGD-modified Ti6Al4V alloy

Table 1. The primer sequences of RT-qPCR

Gene	Primer sequence
Runx2	Forward: 5'-CGGAATGCCTCTGCTGTTATGAA-3' Reverse: 5'-AGGATTTGTGAAGACGGTTATGG-3'
COL I	Forward: 5'-ACAGCCGCTTCACCTACAGC-3' Reverse: 5'-GTTTTGTATTCAATCACTGTCTTGCC-3'
OPN	Forward: 5'- TGA CCA TTC CAA CGA GTC TCA CCA TTC-3' Reverse: 5'- TGG CAT CTG CAC TCT CAA CGT TAG ATC-3'
OCN	Forward: 5'- CAC AGC CTT CGT GTC CAA GC-3' Reverse: 5'- GCT CAG ACA CCT CCC TCC TG-3'
GAPDH	Forward: 5'-GAGTCAACGGATTTGGTCGT-3' Reverse: 5'-TGGGATTTCCATTGATGAAC-3'

as control groups. To determine the effectiveness of E7 modification, the effects of the different Ti6Al4V scaffolds on BMSC adhesion, spreading, and osteogenic differentiation, were analyzed. Development of the E7-modified Ti6Al4V alloy could provide a new approach to improving osseointegration between hip prostheses and host bone.

Materials and methods

Preparation of BMSC affinity peptide and RGD peptide

The BMSC specific affinity peptide (E7) and RGD peptide were commercially synthesized by the Beijing SciLight Biotechnology Ltd. Co. [12]. An L(+)-Cysteine residue was added at the C-terminus of the peptide sequence that was used for covalent attachment in the scaffold functionalization. The peptides were labeled with fluorescein isothiocyanate (FITC) to facilitate detection. E7 and RGD peptides without FITC were also synthesized for immunofluorescence experiments.

Preparation of Ti6Al4V alloy scaffolds

The Ti6Al4V scaffolds (thickness, 2 mm; diameter, 5.5 mm) were derived from a medical Ti6AlV4 rod with a diamond band saw (Exakt, Apparatebau, Germany). To minimize the influence of Ti6Al4V surface roughness, the Ti6Al4V scaffolds were polished to achieve a smooth mirror-like surface with Ra below 40 nm [13]. The Ti6Al4V scaffolds were then successively cleaned with acetone, ethanol, and ultrapure water (20 mins each) in an ultrasonic cleaner. The Ti6Al4V scaffolds were stored at 4°C until used.

Covalent modification of Ti6Al4V scaffolds with peptides

BMSC affinity peptide E7 was conjugated to the surface of Ti6Al4V scaffolds to improve the bio-functionalization (**Figure 1**). The covalent modification procedure was performed according to a previous report [12]. Briefly, the Ti6Al4V scaffolds were immersed in 10% (w/v) 1,6-hexanediamine (Sigma, St. Louis, MO, USA) solution for 60 min at 37°C. After washing with ultrapure water, the aminated Ti6Al4V scaffolds were soaked in 2 mg/mL sulfosuccinimidyl-4-(N-maleimidomethyl) cyclohexane-1-carboxylate (sulfo-SMCC, Thermo Fisher Scientific Inc., Rockford, IL, USA) solution for 60 min at room temperature. The specimens were then incubated in 0.1 mg/mL BMSC affinity peptide solution for 12 h at 4°C. The BMSC affinity peptide-coated Ti6Al4V scaffolds (designated the BTS group) were sterilized and stored at -20°C before use.

A second group of Ti6Al4V scaffolds was fabricated by covalent functionalization with RGD peptide using the same procedure. These scaffolds formed the control group (RTS group). Pure Ti6Al4V scaffolds with no peptide functionalization provided a second control group, designated the PTS group.

Qualitative analysis of BMSC affinity peptide on different scaffolds

Confocal microscopy and scanning electron microscopy (SEM) were used to qualitatively analyze the BMSC affinity peptide on different scaffolds. Briefly, to explore the peptide distribution on different scaffolds, the BTS, RTS, and PTS scaffolds were observed using confocal microscopy at excitation/emission wavelengths of 488/525 nm [14]. Additionally, the BTS, RTS, and PTS scaffolds were analyzed using an SEM equipped with electron dispersive spectroscopy (EDS) to explore their surface topography and composition [15].

Hydrophilic properties of different scaffolds

To explore the hydrophilic properties of the BTS, RTS, and PTS scaffolds, their water contact angles (WCA) were measured [12]. Briefly,

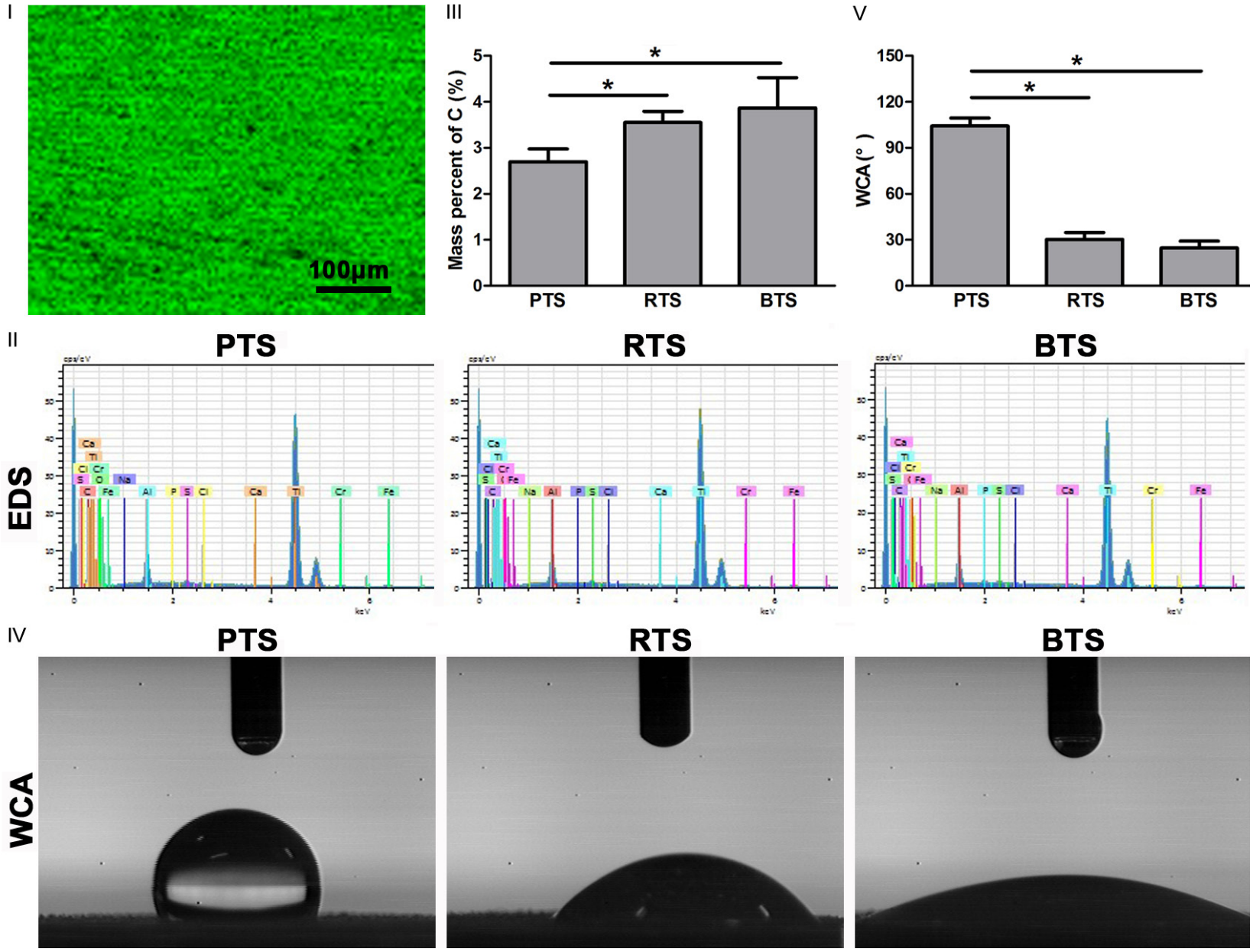
I
100μm
III
Mass percent of C (%)
PTS
RTS
BTS
V
WCA (°)
PTS
RTS
BTS
II
EDS
PTS
RTS
BTS
IV
WCA
PTS
RTS
BTS

Figure 2. Determining the characteristics of E7-modified scaffolds. I. Confocal scanning microscopy image of FITC-E7 peptide modified Ti6Al4V scaffolds. The green fluorescence indicates that E7 was evenly conjugated to the surface of the Ti6Al4V scaffolds. II. EDS spectra of different scaffolds. III. The mass percent of carbon (C) for different scaffolds measured by EDS, indicating that the RTS and BTS scaffolds had higher C content than the PTS scaffold (n = 3, *P < 0.05). IV. Representative images of water contact angle (WCA) for different scaffolds. V. Quantitative analysis of WCA for different scaffolds showing that the RTS and BTS scaffolds were more hydrophilic than the PTS scaffold (n = 3, *P < 0.05).

a drop of water was deposited on the scaffolds and the WCA was measured using a video monitor.

BMSC culture and identification

The BMSCs were acquired from Sprague Dawley (SD) rats (weight, 100 ± 30 g) [10]. The animal study was approved by the ethics commission of Shandong Provincial Hospital affiliated to Shandong University. Briefly, the medulla of the femurs and tibias were carefully flushed with culture media. The specimens were then cultured with alpha-minimum essential medium (α-MEM). After 24 h, the medium was changed to remove the non-adherent cells. Adherent cells were identified as BMSCs by a tri-lineage differentiation experiment (including osteogenic, adipogenic, and chondrogenic differentiation). In detail, to verify the osteogenic differentiation, alizarin red and alkaline phosphatase staining were performed; to verify the adipogenic differentiation, oil red O staining was performed; to verify the chondrogenic differentiation, toluidine blue and collagen II immunohistochemical staining were performed.

BMSC seeding on different scaffolds

Third-passage BMSCs were seeded onto the BTS, RTS, and PTS scaffolds at a density of 3×10^5 cells/cm^2 [16]. Subsequently, the BMSC-loaded scaffolds were incubated with complete α-MEM media at 37°C in a humidified atmosphere (5% CO_2). The cell culture media was changed every 3 d. At specific time points, the BMSC-loaded scaffolds were harvested for various analyses.

Biocompatibility of different scaffolds

To determine the biocompatibility and cytotoxicity of different scaffolds, the BMSCs on different scaffolds were quantified using cell counting kit-8 (CCK-8, Dojindo, Japan) after 1, 3, and 7 d of incubation [17]. Briefly, the BMSC-loaded scaffolds were incubated with 500 μL of CCK-8 solution (1:10 diluted with α-MEM) for 3 h. Subsequently, 100 μL of media from each sample was transferred to a 96-well plate and the absorbance was measured with a microplate reader at a wavelength of 450 nm.

The biological function of BMSC affinity peptide on different scaffolds

To explore the biological function of BMSC affinity peptide E7, the spread of BMSCs on the BTS, RTS, and PTS scaffolds was analyzed by CFM and SEM. For CFM observation, BMSCs on different scaffolds were stained with rhodamine phalloidin (Cytoskeleton Inc., Denver, CO, USA) to label the cytoskeleton [16]. The specimens were then observed using CFM at 544 nm (excitation) and 572 nm (emission). For SEM analysis, the BMSC-loaded scaffolds were immobilized using glutaraldehyde. After desiccation and spraying with gold, the specimens were observed using SEM [18]. To further quantify BMSC bioactivity on different scaffolds, the DNA content was analyzed after incubation for 21 d [16].

In addition, the adhesion force of BMSCs on BTS, RTS, and PTS scaffolds was measured according to previous reports [19, 20]. Briefly, the BMSC-loaded BTS, RTS, and PTS scaffolds were washed with PBS after 1 d to remove the suspended BMSCs, and the number of BMSCs was counted. Subsequently, the BTS, RTS, and PTS scaffolds were centrifuged at 600 and 1000 rpm for 5 min. The ratio of BMSCs adhered to the BTS, RTS, and PTS scaffolds before and after centrifugation was then calculated, allowing the adhesion force of BMSCs on different scaffolds to be calculated.

Osteogenesis of BMSCs on different scaffolds

After allowing BMSCs to seed on scaffolds for 24 h, the BMSC-loaded BTS, RTS, and PTS scaffolds were changed to osteogenic induction media containing 1% glutamine, 0.2% ascorbate, 0.01% dexamethasone, and 1% β-gly-

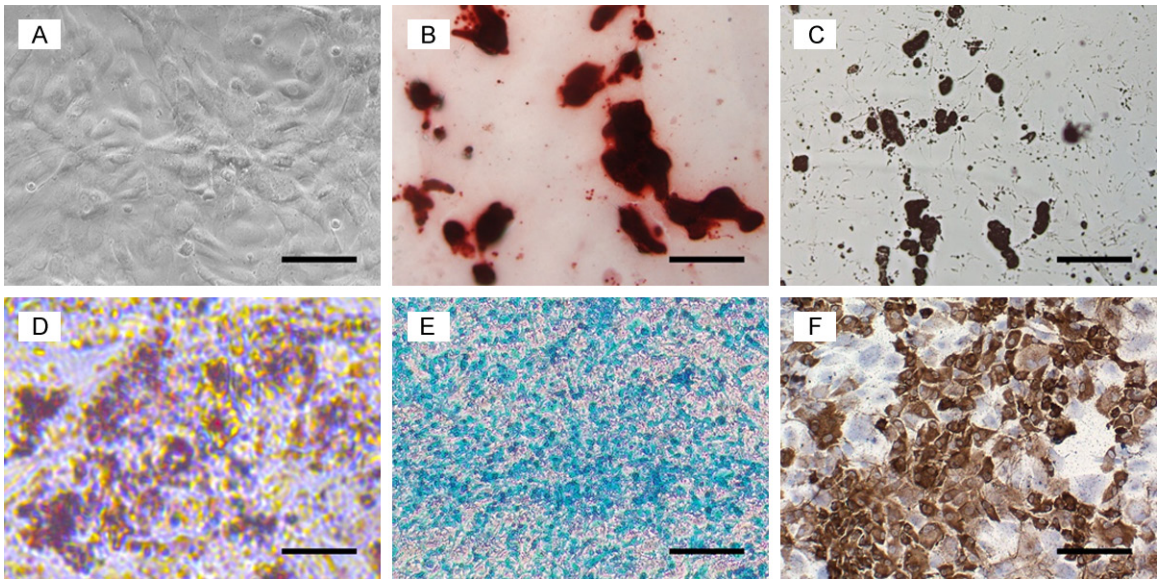

Figure 3. Identification of BMSCs. BMSCs at passage 3 with homogeneous distribution (A). Osteogenesis was verified using alizarin red (B) and alkaline phosphatase staining (C); adipogenesis was examined using oil red O staining (D); chondrogenesis was established using toluidine blue (E) and collagen II immunohistochemical staining (F). (A-F) indicate that BMSCs were successfully cultured. Scale bar = 100 μm.

cerophosphate (Cyagen Biosciences Inc., Goleta, CA, USA) [21]. After 3 weeks of incubation, the specimens were harvested for real-time quantitative PCR (RT-qPCR) and immunofluorescence staining to explore the osteogenesis of BMSCs on different scaffolds.

The RT-qPCR was performed to determine the runt-related transcription factor 2 (Runx2), type I collagen (COL I), osteopontin (OPN), and osteocalcin (OCN) gene expression, which are the markers of BMSC osteogenic differentiation [22]. Briefly, the specimens were immersed in TRIzol reagent to extract total RNA. One microgram of each RNA sample was then used to synthesize complementary DNA (cDNA) with a PrimeScript 1st strand cDNA synthesis kit (TaKaRa, Japan). Finally, quantification of the cDNA was performed using an Applied Biosystems 7300 Real-Time PCR System. The sequences of the oligonucleotide primers are shown in **Table 1**. The mean fold changes of the genes were analyzed using the $2^{-\Delta\Delta Ct}$ method with glyceraldehyde-3-phosphate dehydrogenase (GAPDH) as the reference [23].

Immunofluorescence staining was performed to determine the synthesis of OCN and OPN proteins, which are the specific markers of osteogenesis [24]. To minimize mutual fluorescence interference, the RTS and BTS scaffolds were conjugated with peptides that had not been FITC labeled. Briefly, for the OCN determination, the specimens were incubated in mouse anti-osteocalcin antibody (ab13420; Abcam Inc., Cambridge, MA, USA) for 12 h at 4°C. After rinsing with PBS, the specimens were incubated with goat anti-mouse IgG as the secondary antibody (A11029; Invitrogen, Carlsbad, CA, USA) for 30 min at 37°C. Nuclei were counterstained with Hoechst 33258 (Fanbo Biochemicals Co. Ltd., Beijing, China).

The determination of OPN used the rabbit anti-osteopontin antibody (ab91655; Abcam Inc., Cambridge, MA, USA) as the primary antibody and goat anti-rabbit IgG (A11008; Invitrogen, Carlsbad, CA, USA) as the secondary antibody. The detection procedure for OPN was similar to that of OCN.

Statistical analysis

The statistical significance of the differences among PTS, RTS and BTS scaffolds was analyzed using the analysis of variance (ANOVA) by the SPSS v16.0 software. Mean ± standard deviation was used to express the results. $P < 0.05$ was considered statistically significant. And all of the experiments were performed in triplicate.

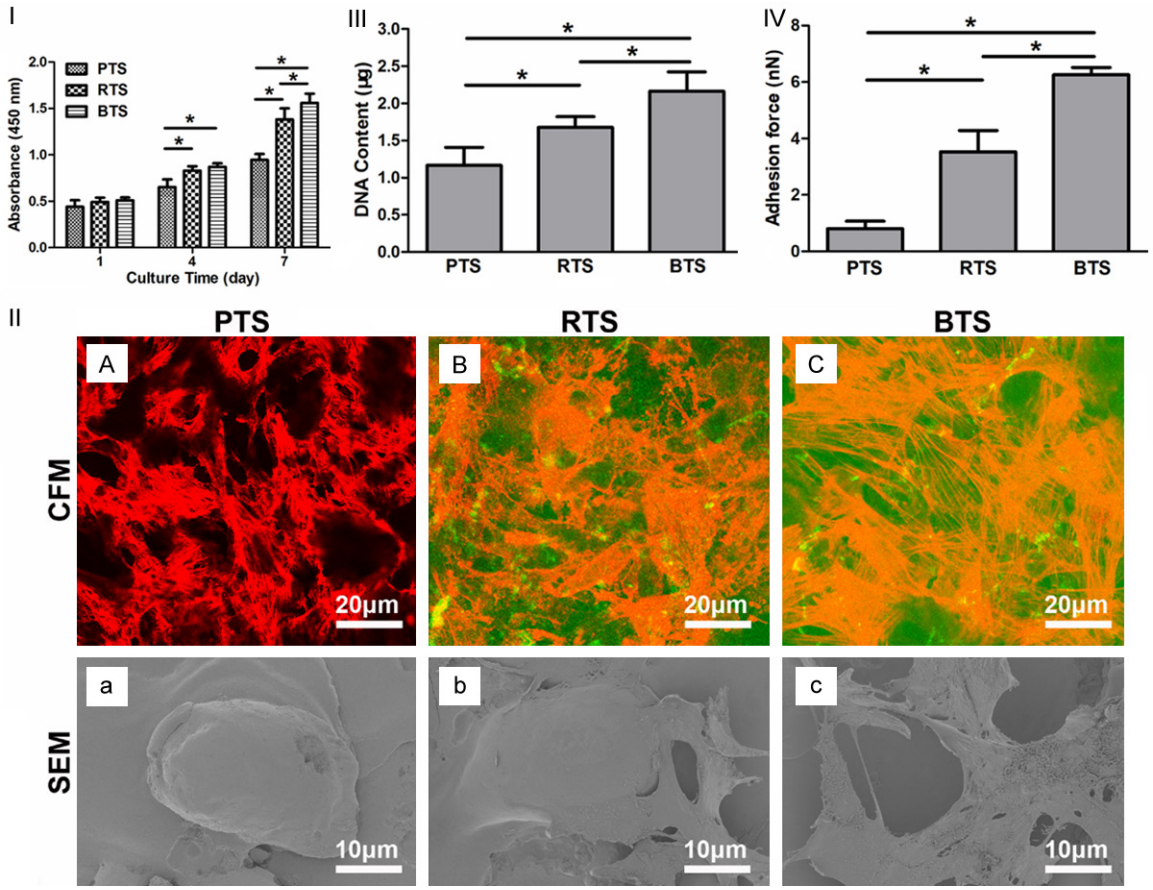

Figure 4. Biocompatibility and bioactivity of BTS scaffolds. (I) BMSC survival on different scaffolds was measured using a CCK-8 kit. The BMSCs proliferated with time, indicating that the PTS, RTS, and BTS scaffolds showed no cytotoxicity. (II) Spreading of BMSCs on different scaffolds after incubation for 24 h. Images (A), (B), and (C) show the confocal scanning of cytoskeleton staining for BMSCs. BMSCs on the BTS scaffolds exhibited better spreading morphology than those on the RTS and PTS scaffolds. Red, rhodamine phalloidin; green, FITC-labeled RGD or E7. Images a, b, and c show the SEM scanning of BMSC spreading. BMSCs of the BTS group expanded better than the two other groups, which was consistent with the results of cytoskeleton staining (A-C). (III) The adhesion force of BMSCs on different scaffolds. The results indicate that BMSCs on the BTS scaffolds had stronger adhesion force than those of other groups. (IV) DNA content of different groups after 21 d incubation. The results indicate that BMSCs on the BTS scaffolds had better bioactivity than those of other groups (n = 3, *P < 0.05).

Results

Covalent modification of Ti6Al4V scaffold with BMSC affinity peptide E7

To confirm the successful covalent modification of Ti6Al4V scaffold with BMSC affinity peptide E7, the BTS scaffolds were observed using confocal microscopy. As shown in **Figure 2I**, FITC-modified E7 was evenly distributed on the surface of the Ti6Al4V, indicating that the BTS scaffolds were successfully fabricated.

To further confirm the conjugation of the peptides to Ti6Al4V, EDS was carried out. As shown in **Figure 2II**, **2III**, the mass percent of carbon for the RGD-modified scaffold (RTS) and BTS scaffold were significantly higher than that of the unmodified Ti6Al4V scaffold (PTS). This result supports the successful conjugation of the peptides to the Ti6Al4V alloy because both peptides contain carbon.

Hydrophilic properties of BTS scaffolds

The hydrophilic properties of the different scaffolds were demonstrated using water contact angle. As shown in **Figure 2IV**, **2V**, the BTS and RTS scaffolds were more hydrophilic than the PTS scaffold. There was no significant difference between the hydrophilicity of the BTS and RTS scaffolds.

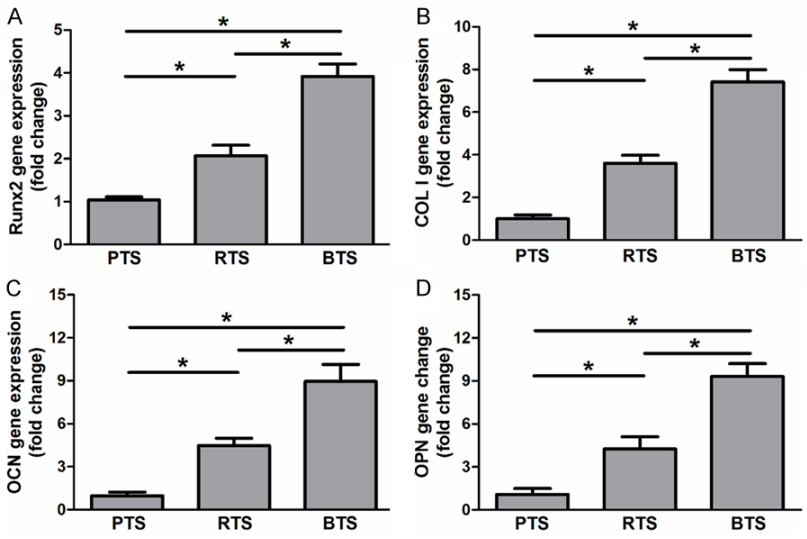

Figure 5. Expression of osteogenic genes for BMSCs on different scaffolds determined by RT-qPCR after incubation for 21 d. (A) Runx2 gene; (B) COL I gene; (C) OCN gene; (D) OPN gene (n = 3, *P < 0.05). (A-D) show that the expression of osteogenic genes for BMSCs on the BTS scaffolds was significantly higher than for the other groups.

BMSC culture and identification

BMSCs were extracted from Sprague Dawley (SD) rats, and their properties were determined using a tri-lineage differentiation experiment. As shown in **Figure 3**, alizarin red and ALP staining indicated that the BMSCs could be differentiated into osteoblast-like cells; the Oil Red O staining indicated that the BMSCs could be induced into adipocytes; and the Alcian blue and collagen II staining indicated that the BMSCs could be induced into chondrocytes (**Figure 3**). Taken together, these results demonstrate that the BMSCs were successfully cultured, and had the potential for multi-lineage differentiation.

BTS scaffolds show no cytotoxicity

CCK-8 analysis was performed to determine the biocompatibility and cytotoxicity of the PTS, RTS, and BTS scaffolds. As shown in **Figure 4I**, the BMSCs proliferated with time in all cases, indicating that the scaffolds showed no cytotoxicity. From the fourth day of incubation, the absorbance for the PTS group was significantly lower than those of the BTS and RTS groups, which might be due to the lack of functional peptides on the PTS scaffolds. After incubation for 7 d, the absorbance in the BTS group was significantly higher than that in the RTS group, which could indicate that the E7 peptide has superior affinity for BMSCs than the RGD peptide.

Biological function of E7 on BTS scaffolds

To determine the biological function of E7, cell morphology and DNA content were analyzed. As shown in **Figure 4IIA-C**, the BMSCs on the BTS scaffolds showed better spreading than the other two groups after 24 h of incubation. In addition, the cell morphology observed by SEM showed that the BMSCs of the BTS group expanded better than those of the two other groups (**Figure 4IIA-C**), which was consistent with the results of cytoskeleton staining. The adhesion force of BMSCs on the BTS scaffolds was also stronger than for the other groups (**Figure 4III**). After incubation for 21 d, the DNA content of the BTS group was significantly higher than those of the PTS and RTS groups (**Figure 4IV**), which indicates that BMSCs on the BTS scaffolds had better bioactivity than those in the other groups. From these data it can be concluded that the E7 on the BTS scaffold can efficiently promote BMSC adhesion.

Osteogenic performance of BMSCs on different scaffolds

Analysis of the osteogenic performance of BMSCs on different scaffolds was carried out using RT-qPCR and immunofluorescence staining to quantify the specific osteogenesis markers. As shown in **Figure 5**, after incubation for 21 d, the expression of Runx2, COL I, OCN, and OPN genes in the BTS group was significantly greater than those for the RTS and PTS groups.

Immunofluorescence staining showed that the synthesis of OCN and OPN proteins in the BTS group was significantly higher than in the RTS and PTS groups (**Figure 6**), which supported the results of RT-qPCR.

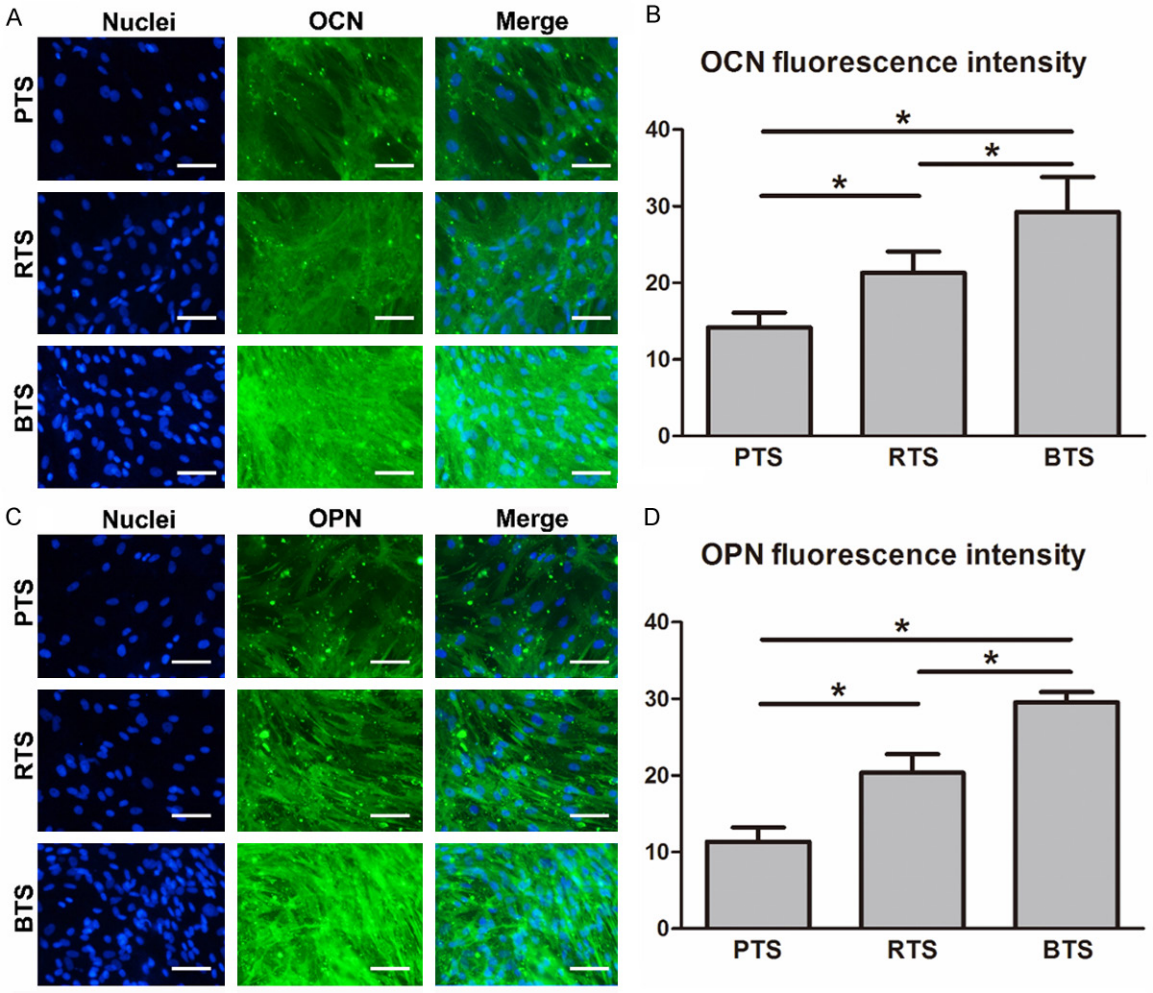

Figure 6. Synthesis of osteogenic proteins for BMSCs on different scaffolds determined by immunofluorescence staining after incubation for 21 d. A. Representative images of OCN immunofluorescence staining (Scale bar = 25 μm); B. Analysis of OCN fluorescence intensity with Image-Pro Plus 6.0 software showed that more OCN was synthesized in the BTS group (n = 3, *P < 0.05); C. Representative images of OPN immunofluorescence staining (Scale bar = 25 μm); D. The analysis of OPN fluorescence intensity with Image-Pro Plus 6.0 software indicates that more OPN was synthesized in the BTS groups (n = 3, *P < 0.05).

Discussion

Ti6Al4V alloy has been widely used for hip joint prostheses because of its proven biocompatibility and mechanical properties [1]. However, Ti6Al4V lacks a biomimetic surface to promote efficient osseointegration, which often leads to looseness of joint prostheses [2]. It is known that BMSCs play an important role in the osseointegration between host bone and joint prostheses because osteoblasts in the periprosthetic site are differentiated from BMSCs [7]. Therefore, enriching the concentration of BMSCs at the periprosthetic site could be a promising approach to improving the osseointegration between host bone and joint prostheses [8]. In the current study, we conjugated the BMSC specific affinity peptide, E7, to Ti6Al4V alloy to improve the bioactivity of the Ti6Al4V surface.

As shown in **Figure 2I-III**, the E7 was evenly conjugated to the Ti6Al4V alloy, indicating that the BTS scaffold could be successfully fabricated. In addition, conjugation of E7 led to an increase in the hydrophilicity of the BTS scaffolds compared with the PTS group (**Figure 2IV-V**). The increased hydrophilicity could promote nutritional exchange for BMSCs adhered to the scaffolds [25], which might improve the osteogenesis of BMSCs on the BTS scaffolds.

The biological function of E7 on the BTS scaffolds was further investigated, with CCK-8 experiments showing that the BMSCs on the BTS scaffold proliferated with time (**Figure 4I**), indicating that the BTS scaffolds were not cytotoxic. Importantly, the BTS scaffolds supported better BMSC spreading and adhesion force than the other groups (**Figure 4II-III**), which was consistent with a previous report [6]. After incubation for 21 d, the DNA content in the BTS group was significantly higher than those in the PTS and RTS groups (**Figure 4IV**), which indicated that BMSCs on the BTS scaffolds had better bioactivity than those on the other surfaces. From these data, we conclude that the BTS scaffolds could efficiently improve the adhesion of BMSCs, which could be due to the conjugation of BMSC affinity peptide E7.

In addition, the osteogenic performance of BMSCs on BTS scaffolds was analyzed using RT-qPCR and immunofluorescence staining. Both results indicated that the biomimetic BTS scaffolds were more conducive to osteogenesis than the other scaffolds (**Figures 5** and **6**). The reason for the better osteogenic performance of the BTS scaffolds may be that BMSCs show better adhesion and spreading under these conditions, which is attributed to the BMSC specific affinity peptide E7 on the surface of the scaffolds (**Figure 4**). Previous studies have reported that the adhesion of seed cells on scaffolds is the first step of cell-scaffold interaction in tissue engineering, and the state of adhesion affects the subsequent biological function of cells [26]. Consequently, the enhanced initial adhesion of BMSCs to BTS scaffolds could be conducive to the subsequent osteogenesis of BMSCs.

In addition, the enhanced adhesion of BMSCs to BTS compared with other scaffolds, might also decrease the infection rate. Infection is a catastrophic complication for hip arthroplasty [9], and reducing infection rate is therefore a priority. Previous studies have reported that a "race for the surface" between bacteria and tissue cells takes place immediately following implantation of a prosthesis in hip arthroplasty [10]. If bacteria win the race, hip periprosthetic joint infection may occur. The biomimetic BTS scaffolds, which support the adhesion of seed cells during the "race for the surface", might help to decrease the infection rate [11].

In this study, we constructed a functional BTS scaffold modified with BMSC specific affinity peptide E7, which specifically promoted the adhesion and spreading of BMSCs. When cultured with osteogenic induction medium, the BMSCs on BTS scaffolds show better osteogenic performance than the controls, which could be attributed to the superior initial adhesion of BMSCs to the BTS scaffolds. The functional BTS scaffold could pave the way for designing functional joint prostheses that promote osseointegration between the host bone and prosthesis. However, the *in vivo* biological function of BTS scaffolds and the specific mechanism of E7 in improving BMSC adhesion, have not been ascertained and will be explored in future work.

Acknowledgements

The authors gratefully acknowledge the support from the National Natural Science Foundation of China (Grant Nos 30672115, 81672185 and 81702152), the Natural Science Foundation of Shandong province (Grant No ZR2017BH015), and the science and technology development plan of Shandong Province (Grant Nos 2012GSF21809 and 2017GSF218025).

Disclosure of conflict of interest

None.

Address correspondence to: Wei Li, Department of Joint Surgery, Shandong Provincial Hospital Affiliated to Shandong University, Jinan 250021, Shandong Province, P. R. China. E-mail: greatli2000@163.com

References

[1] Mas-Moruno C, Dorfner PM, Manzenrieder F, Neubauer S, Reuning U, Burgkart R and Kessler H. Behavior of primary human osteoblasts on trimmed and sandblasted Ti6Al4V surfaces functionalized with integrin alphavbeta3-selective cyclic RGD peptides. J Biomed Mater Res A 2013; 101: 87-97.

[2] Li X, Gao P, Wan P, Pei Y, Shi L, Fan B, Shen C, Xiao X, Yang K and Guo Z. Novel bio-functional magnesium coating on porous Ti6Al4V orthopaedic implants: in vitro and in vivo study. Sci Rep 2017; 7: 40755.

[3] Schickle K, Gerardo-Nava JL, Puidokas S, Anavar SS, Bergmann C, Gingter P, Schickle B, Bobzin K and Fischer H. Preparation of spherical calcium phosphate granulates suitable for the biofunctionalization of active brazed tita-

nium alloy coatings. Biomed Tech (Berl) 2015; 60: 105-114.
[4] Migita S, Okuyama S and Araki K. Sub-micrometer scale surface roughness of titanium reduces fibroblasts function. J Appl Biomater Funct Mater 2016; 14: e65-69.
[5] Felgueiras HP, Sommerfeld SD, Murthy NS, Kohn J and Migonney V. Poly(NaSS) functionalization modulates the conformation of fibronectin and collagen type I to enhance osteoblastic cell attachment onto Ti6Al4V. Langmuir 2014; 30: 9477-9483.
[6] Shao Z, Zhang X, Pi Y, Wang X, Jia Z, Zhu J, Dai L, Chen W, Yin L, Chen H, Zhou C and Ao Y. Polycaprolactone electrospun mesh conjugated with an MSC affinity peptide for MSC homing in vivo. Biomaterials 2012; 33: 3375-3387.
[7] Holt G, Murnaghan C, Reilly J and Meek RM. The biology of aseptic osteolysis. Clin Orthop Relat Res 2007; 460: 240-52.
[8] Shen Y, Li X, Ding Y, Ren W and Wang W. Stro-1-positive BMSCs predict postoperative periprosthetic bone mineral density outcomes in uncemented total hip arthroplasty patients. Med Sci Monit 2014; 20: 361-367.
[9] Grammatopoulos G, Bolduc ME, Atkins BL, Kendrick BJ, McLardy-Smith P, Murray DW, Gundle R and Taylor AH. Functional outcome of debridement, antibiotics and implant retention in periprosthetic joint infection involving the hip: a case-control study. Bone Joint J 2017; 99-B: 614-622.
[10] Gristina AG. Biomaterial-centered infection: microbial adhesion versus tissue integration. Science 1987; 237: 1588-1595.
[11] Poth N, Seiffart V, Gross G, Menzel H and Dempwolf W. Biodegradable chitosan nanoparticle coatings on titanium for the delivery of BMP-2. Biomolecules 2015; 5: 3-19.
[12] Meng Q, Hu X, Huang H, Liu Z, Yuan L, Shao Z, Jiang Y, Zhang J, Fu X, Duan X and Ao Y. Microfracture combined with functional pig peritoneum-derived acellular matrix for cartilage repair in rabbit models. Acta Biomater 2017; 53: 279-292.
[13] Hoyos-Nogues M, Velasco F, Ginebra MP, Manero JM, Gil FJ and Mas-Moruno C. Regenerating bone via multifunctional coatings: the blending of cell integration and bacterial inhibition properties on the surface of biomaterials. ACS Appl Mater Interfaces 2017; 9: 21618-21630.
[14] Man Z, Sha D, Sun S, Li T, Li B, Yang G, Zhang L, Wu C, Jiang P, Han X and Li W. In vitro bioactivity study of RGD-coated titanium alloy prothesis for revision total hip arthroplasty. Biomed Res Int 2016; 2016: 8627978.
[15] Miola M, Fucale G, Maina G and Verne E. Antibacterial and bioactive composite bone cements containing surface silver-doped glass particles. Biomed Mater 2015; 10: 055014.
[16] Man Z, Yin L, Shao Z, Zhang X, Hu X, Zhu J, Dai L, Huang H, Yuan L, Zhou C, Chen H and Ao Y. The effects of co-delivery of BMSC-affinity peptide and rhTGF-beta1 from coaxial electrospun scaffolds on chondrogenic differentiation. Biomaterials 2014; 35: 5250-5260.
[17] Lu LX, Zhang XF, Wang YY, Ortiz L, Mao X, Jiang ZL, Xiao ZD and Huang NP. Effects of hydroxyapatite-containing composite nanofibers on osteogenesis of mesenchymal stem cells in vitro and bone regeneration in vivo. ACS Appl Mater Interfaces 2013; 5: 319-330.
[18] Zhang HX, Xiao GY, Wang X, Dong ZG, Ma ZY, Li L, Li YH, Pan X and Nie L. Biocompatibility and osteogenesis of calcium phosphate composite scaffolds containing simvastatin-loaded PLGA microspheres for bone tissue engineering. J Biomed Mater Res A 2015; 103: 3250-3258.
[19] Reyes CD and Garcia AJ. A centrifugation cell adhesion assay for high-throughput screening of biomaterial surfaces. J Biomed Mater Res A 2003; 67: 328-333.
[20] Li Q, Xing D, Ma L and Gao C. Synthesis of E7 peptide-modified biodegradable polyester with the improving affinity to mesenchymal stem cells. Mater Sci Eng C Mater Biol Appl 2017; 73: 562-568.
[21] Poh PSP, Hutmacher DW, Holzapfel BM, Solanki AK, Stevens MM and Woodruff MA. In vitro and in vivo bone formation potential of surface calcium phosphate-coated polycaprolactone and polycaprolactone/bioactive glass composite scaffolds. Acta Biomater 2016; 30: 319-333.
[22] Zhou Y, Wu Y, Jiang X, Zhang X, Xia L, Lin K and Xu Y. The effect of quercetin on the osteogenesic differentiation and angiogenic factor expression of bone marrow-derived mesenchymal stem cells. PLoS One 2015; 10: e0129605.
[23] Livak KJ and Schmittgen TD. Analysis of relative gene expression data using real-time quantitative PCR and the 2(-Delta Delta C(T)) Method. Methods 2001; 25: 402-408.
[24] Strauss S, Dudziak S, Hagemann R, Barcikowski S, Fliess M, Israelowitz M, Kracht D, Kuhbier JW, Radtke C, Reimers K and Vogt PM. Induction of osteogenic differentiation of adipose derived stem cells by microstructured nitinol actuator-mediated mechanical stress. PLoS One 2012; 7: e51264.
[25] Grafahrend D, Heffels KH, Beer MV, Gasteier P, Moller M, Boehm G, Dalton PD and Groll J. Degradable polyester scaffolds with controlled surface chemistry combining minimal protein adsorption with specific bioactivation. Nat Mater 2011; 10: 67-73.
[26] Anselme K. Osteoblast adhesion on biomaterials. Biomaterials 2000; 21: 667-681.